An Analytical Time–Domain Expression for the Net Ripple Produced by Parallel Interleaved Converters

Brian B. Johnson, *Member, IEEE*, and Philip T. Krein, *Fellow, IEEE*

***Abstract*—We apply modular arithmetic and Fourier series to analyze the superposition of N interleaved triangular waveforms with identical amplitudes and duty ratios. Here, interleaving refers to the condition when a collection of periodic waveforms with identical periods is uniformly phase shifted across one period. The main result is a time–domain expression that provides an exact representation of the summed and interleaved triangular waveforms, where the peak amplitude and parameters of the time-periodic component are all specified in closed form. Analysis is general and can be used to study various applications in multi-converter systems. This model is unique not only in that it reveals a simple and intuitive expression for the net ripple, but its derivation via modular arithmetic and Fourier series is distinct from prior approaches. The analytical framework is experimentally validated with a system of three parallel converters under time-varying operating conditions.**

***Index Terms*—DC–DC converters, Fourier analysis, interleaving, inverters, modular arithmetic, parallel converters.**

I. Introduction

As POWER electronics interfaces become increasingly pervasive across applications, energy delivery systems are evolving toward progressively distributed architectures. In contrast to centralized structures, multiconverter systems allow for the coordination of many controllable circuits to achieve various types of objectives such as load sharing, converter synchronization, and harmonic mitigation. From here forward, we focus on the objective of ripple cancellation through a technique called switch interleaving. This method is based on staggering the switch transitions of many parallel converters so that the current ripple of each converter undergoes cancellation once summed together at a common load. In this brief, we apply notions from modular arithmetic and Fourier series to develop a novel analytic time–domain model and show that the superposition of N interleaved triangular waveforms is exactly equal to another single triangular waveform whose net amplitude, effective duty ratio, and effective frequency can be specified in terms of the original parameters in closed form. The presented model also encapsulates the time–domain behavior of the net waveform and is experimentally validated on a system of three parallel converters.

Ripple cancellation and interleaving in converter systems has a rich history in the power electronics literature [1]–[4]. Some of the earliest efforts on developing an analytical model can be found in [5] and [6] where multiple cancellation factors were computed that yield the net ripple amplitude once multiplied together. However, because these expressions were not in closed form and required numerical operations for their computation, a compact and intuitive mathematical description was eluded. Related approaches based on numerical methods [7] were further investigated over the next several years.

In general, Fourier transforms and series have been applied in various contexts to shed further light on the mathematical properties of ripple cancellation. For instance, Fourier methods were applied in [8] to study interleaving in various engineering applications. However, the reported expressions only apply in specific cases and are not applicable for generalized duty ratios and N. Additional characterizations using Fourier series appear in works such as [9], but a general expression is not obtained. With respect to more recent efforts, phasor-based methods were applied in [10] and [11] to study the effect of nonuniform waveform characteristics in interleaved systems. Finally, floor and ceiling functions were utilized in [12] to provide an alternate framework for analysis.

Formulations in the existing literature have one or more of the following drawbacks: i) The amplitude of the net-ripple waveform is not obtained in closed form; ii) ripple characteristics are often estimated with numerical methods [5], [7]; and iii) representations of the net ripple amplitude [11], [12] are presented in a format that obscures an intuitive interpretation. In summary, prior works lack an exact time–domain model with all parameters given in closed form. In contrast, we derive a model of the net ripple generated by N interleaved parallel converters where all parameters are specified in closed form, and the resulting expression is presented in a simple form that straightforwardly shows how ripple cancellation is a function of the number of parallel converters, N, and the instantaneous duty ratio d. From an analytical standpoint, the presented formulation is distinctive from existing methods in that we

Manuscript received April 5, 2016; accepted April 10, 2016. Date of publication April 21, 2016; date of current version February 24, 2017. The work of B. B. Johnson was supported in part by the Laboratory Directed Research and Development program at NREL and in part by the U.S. Department of Energy under Contract DE-AC36-08-GO28308 with National Renewable Energy Laboratory (NREL). The work of P. T. Krein was supported in part by the Grainger Center for Electric Machinery and Electromechanics at the University of Illinois and in part by the Mid-America Regional Microgrid Education and Training Consortium headquartered at Missouri University of Science and Technology. This brief was recommended by Associate Editor X. Ruan.

B. B. Johnson is with the Power Systems Engineering Center, National Renewable Energy Laboratory, Golden, CO 80401 USA (e-mail: brian.johnson@nrel.gov).

P. T. Krein is with the Department of Electrical and Computer Engineering, University of Illinois, Urbana, IL 61801 USA (e-mail: krein@illinois.edu).

Color versions of one or more of the figures in this brief are available online at http://ieeexplore.ieee.org.

Digital Object Identifier 10.1109/TCSII.2016.2557620

1549-7747 © 2016 IEEE. Personal use is permitted, but republication/redistribution requires IEEE permission.
See http://www.ieee.org/publications_standards/publications/rights/index.html for more information.

Authorized licensed use limited to: University of Washington Libraries. Downloaded on February 10,2022 at 21:47:26 UTC from IEEE Xplore. Restrictions apply.

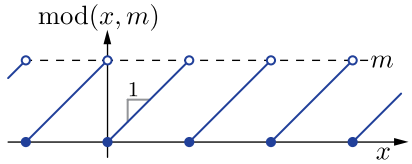

Fig. 1. Modulo operator with input signal x evaluated with modulus m.

leverage both modular arithmetic and Fourier series to arrive at it. Finally, the time–domain model is validated experimentally under time-varying conditions to show its effectiveness in modeling real-time operation.

From here forward, Section II covers notation and fundamentals, and Section III contains the main result. An experimental validation of the proposed time–domain formulation is given in Section IV. Concluding statements are in Section V.

II. Preliminaries

A. Notation

The sets of real and complex numbers are denoted as $\mathbb{R}$ and $\mathbb{C}$, respectively, and $\mathbb{R}_{>0}$ is the set of positive real numbers. $\mathbb{Z}$ denotes the set of real integers. The imaginary unit is given as $j = \sqrt{-1}$. We utilize notions from *modular arithmetic*, oftentimes called *clock arithmetic*, where numbers "wrap around" zero and another number called the *modulus*. Given a number $x \in \mathbb{R}$, the floor function, denoted as $\lfloor x \rfloor$, yields the largest integer less than or equal to x. Essentially, the floor function rounds down to the nearest integer. It then follows that $x - m\lfloor x/m \rfloor$ is equal to the *remainder* after the division of x by m. For compactness, we borrow notation commonly used in computer languages and introduce the modulo operator, $\mathrm{mod} : \mathbb{R} \times \mathbb{R}_{>0} \to \mathbb{R}_{>0}$, which is defined as $\mathrm{mod}(x, m) := x - m\lfloor x/m \rfloor$. When utilizing the modulo operator as $\mathrm{mod}(x, m)$, we consider x as an input signal and refer to $m > 0$ as the *modulus*, which acts as a positive upper limit on the operator output. As shown in Fig. 1, the "wrap-around" behavior of the modulo operator is apparent.

For ease of exposition, we define the time-periodic triangular function $f_{\mathrm{tri}} : \mathbb{R} \times \mathbb{R}_{>0} \times \mathbb{R}_{>0} \to \mathbb{R}$, which is shown in Fig. 2 and its output over one period is

$$f_{\mathrm{tri}}(t - \phi, d, T) = \begin{cases} 1 - \frac{2}{(1-d)T}(t - \phi) & \text{for } 0 \le t - \phi \le (1-d)T \\ \frac{d-2}{d} + \frac{2}{dT}(t - \phi) & \text{for } (1-d)T \le t - \phi \le T. \end{cases} \quad (1)$$

f_{tri} is parameterized by its phase shift ϕ, duty ratio d, and period T. The function $f_{\mathrm{tri}}(t - \phi, d, T)$ has unity peak amplitude over each cycle, and the duration of time within each cycle where the slope is positive is equal to dT. Here, we use the term *duty ratio*, $d \in (0, 1)$, to denote the fraction of the period over which the waveform slope is positive. Since $f_{\mathrm{tri}}(t - \phi, d, T)$ is periodic, Fourier analysis can be applied to attain the following infinite series:

$$f_{\mathrm{tri}}(t - \phi, d, T) = \sum_{n=1}^{\infty} \frac{2\sin(n\pi d)}{n^2\pi^2 d(1-d)} \sin\left(\frac{2n\pi}{T}(t - \phi) + n\pi d\right). \quad (2)$$

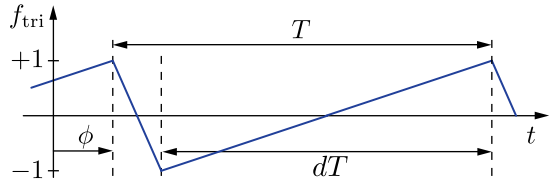

Fig. 2. Periodic triangular waveform with unity amplitude, period T, duty ratio d, and phase shift ϕ will be denoted as $f_{\mathrm{tri}}(t - \phi, d, T)$.

B. Problem Statement

Analysis is focused on systems of N triangular current waveforms where the kth waveform is of the form

$$i_k = I f_{\mathrm{tri}}(t - \phi_k, d, T). \quad (3)$$

We seek an analytical representation for the superposition of N interleaved triangular current waveforms with identical amplitudes. Given N periodic current waveforms with amplitude I, period T, and duty ratio d, the term *interleaved* refers to condition when the kth waveform is phase shifted by $\phi_k = kT/N$ for $k = 0, \ldots, N-1$.

III. Analysis of Interleaved Triangular Waveforms

In this section, we put forward the main result of this brief. Specifically, we first present an analytical expression for the summation of N interleaved current waveforms. Utilizing Fourier series and modular arithmetic, we prove that this summation may be expressed as the product of a net amplitude $\bar{I}$ and another triangular waveform.

Theorem 1: The superposition of N interleaved triangular current waveforms, each with amplitude I, duty ratio d, and period T, is given by

$$\sum_{k=0}^{N-1} I f_{\mathrm{tri}}\left(t - \frac{kT}{N}, d, T\right) = \bar{I} f_{\mathrm{tri}}(t, \bar{d}, \bar{T}) \quad (4)$$

where the net amplitude is given by

$$\bar{I} = I\frac{\mathrm{mod}(Nd, 1)\,(1 - \mathrm{mod}(Nd, 1))}{Nd(1-d)} \quad (5)$$

the effective duty ratio is

$$\bar{d} = \mathrm{mod}(Nd, 1) \quad (6)$$

and the effective switching period is equal to

$$\bar{T} = \frac{T}{N}. \quad (7)$$

Proof: The proof consists of two parts. In the first portion, we show that the amplitude of the net current waveform is given by (5). Next, the triangular function on the right-hand side of (4) is derived such that (6) and (7) are also validated.

Authorized licensed use limited to: University of Washington Libraries. Downloaded on February 10,2022 at 21:47:26 UTC from IEEE Xplore. Restrictions apply.

1) Amplitude of Net Waveform: We begin by dividing both sides of (4) by I and substituting (2) in (4) to obtain

$$\begin{aligned}
&\sum_{k=0}^{N-1} f_{\mathrm{tri}}\left(t-\frac{kT}{N},d,T\right)\\
&=\sum_{k=0}^{N-1}\sum_{n=1}^{\infty}\frac{2\sin(n\pi d)}{n^2\pi^2 d(1-d)}\sin\left(\frac{2n\pi}{T}\left(t-\frac{kT}{N}\right)+n\pi d\right)\\
&=\sum_{n=1}^{\infty}\frac{2\sin(n\pi d)}{n^2\pi^2 d(1-d)}\sum_{k=0}^{N-1}\sin\left(\frac{2n\pi}{T}\left(t-\frac{kT}{N}\right)+n\pi d\right)\\
&=\sum_{n=1}^{\infty}\frac{2\sin(Nn\pi d)}{N^2n^2\pi^2 d(1-d)}\sum_{k=0}^{N-1}\sin\left(\frac{2Nn\pi}{T}t+Nn\pi d\right)\\
&=\sum_{n=1}^{\infty}\underbrace{\frac{2\sin(Nn\pi d)}{Nn^2\pi^2 d(1-d)}}_{:=c_n}\sin\left(\frac{2Nn\pi}{T}t+Nn\pi d\right) \qquad (8)
\end{aligned}$$

where the second line follows from a rearrangement of terms. The third line emerges from the following property: $\sum_{k=1}^{k=N-1}\sin(2n\pi(t-kT/N)/T)=0,\quad \forall n\in\{n|\mathrm{mod}(n/N,N)\neq 0\}$. In other words, summations over $k=0,\ldots,N-1$ are nonzero if and only if n is an integer multiple of N (i.e., $\mathrm{mod}(n/N,N)=0$). Accordingly, summation indices over n can be multiplied by N to capture nonzero terms, and the dependence on k can be eliminated.

By comparison, it is evident that (8) takes the same form as (2). Hence, the waveform in (8) is also triangular. Next, we leverage the relationship between the peak amplitude and cycle root mean square (RMS) of a triangular waveform as given by $A_{\mathrm{pk}}=\sqrt{3}A_{\mathrm{rms}}$, where A_{pk} and A_{rms} denote the peak amplitude and cycle RMS. Recall that the RMS of a waveform with the form in (8) is equal to $(\sum_{n=1}^{\infty}c_n^2/2)^{1/2}$. Thus, the peak amplitude is given by

$$\begin{aligned}
\frac{\bar{I}}{I}&=\sqrt{\frac{3}{2}\sum_{n=1}^{\infty}c_n^2}\\
&=\sqrt{\frac{3}{2}\sum_{n=1}^{\infty}\frac{4\sin^2(Nn\pi d)}{N^2n^4\pi^4 d^2(1-d)^2}}\\
&=\frac{\sqrt{6}}{N\pi^2 d(1-d)}\sqrt{\sum_{n=1}^{\infty}\frac{1}{2}\frac{(1-\cos(2Nn\pi d))}{n^4}} \qquad (9)
\end{aligned}$$

where, in the last line, we utilize the double angle formula. The following series can be written in closed form [13] as:

$$\sum_{n=1}^{\infty}\frac{\cos(nx)}{n^4}=\frac{\pi^4}{90}-\frac{\pi^2x^2}{12}+\frac{\pi x^3}{12}-\frac{x^4}{48},\ 0\le x\le 2\pi \qquad (10)$$

$$\sum_{n=1}^{\infty}\frac{1}{n^4}=\frac{\pi^4}{90}. \qquad (11)$$

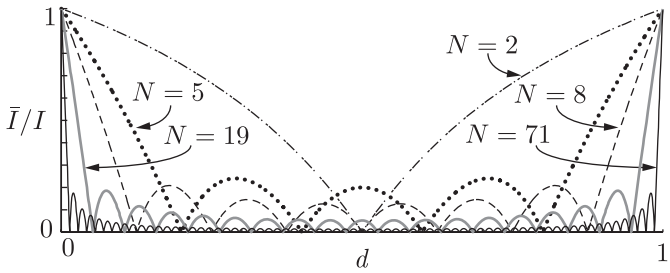

Fig. 3. Ripple cancellation factor as a function of duty ratio for several values of N. The illustrated curves are computed using (5).

Applying (10) and (11) and utilizing the modulo operator to ensure $0\le 2N\pi d\le 2\pi$ as dictated by (10), (9) becomes

$$\begin{aligned}
&\sum_{n=1}^{\infty}\frac{1}{2}\frac{(1-\cos(2Nn\pi d))}{n^4}\\
&\quad=\frac{1}{2}\left(\frac{\pi^2\mathrm{mod}^2(2N\pi d,2\pi)}{12}-\frac{\pi\mathrm{mod}^3(2N\pi d,2\pi)}{12}\right.\\
&\qquad\left.+\frac{\mathrm{mod}^4(2N\pi d,2\pi)}{48}\right)\\
&\quad=\frac{\pi^4}{6}\mathrm{mod}^2(Nd,1)\left(1-\mathrm{mod}(Nd,1)\right)^2. \qquad (12)
\end{aligned}$$

Substituting (12) into (9) yields the expression in (5), thus completing the first part of the proof.

2) Duty Ratio and Frequency of Net Triangular Component: Dividing both sides of (4) by $\bar{I}$ and substituting (8) and the result of the first part of the proof, as summarized in (5), we obtain

$$\begin{aligned}
&f_{\mathrm{tri}}(t,\bar{d},\bar{T})\\
&\quad=\frac{Nd(1-d)}{\mathrm{mod}(Nd,1)\left(1-\mathrm{mod}(Nd,1)\right)}\\
&\qquad\times\sum_{n=1}^{\infty}\frac{2\sin(Nn\pi d)}{Nn^2\pi^2 d(1-d)}\sin\left(\frac{2Nn\pi}{T}t+Nn\pi d\right)\\
&\quad=\sum_{n=1}^{\infty}\frac{2\sin\left(n\pi\mathrm{mod}(Nd,1)\right)}{n^2\pi^2\mathrm{mod}(Nd,1)\left(1-\mathrm{mod}(Nd,1)\right)}\\
&\qquad\times\sin\left(\frac{2n\pi}{T/N}t+n\pi\mathrm{mod}(Nd,1)\right) \qquad (13)
\end{aligned}$$

where the final expression arises from the fact that $\sin(Nn\pi d)\sin(x+Nn\pi d)$ and $\sin(n\pi\mathrm{mod}(Nd,1))\sin(x+n\pi\mathrm{mod}(Nd,1))$ are exactly equal $\forall\, x\in\mathbb{R}$, which, in turn, follows from the π periodicity of a product of two sinusoids with identical frequencies. Applying (2) to (13) and referring to the right-hand side of (4), we indeed see that (6) and (7) are validated. This completes the proof. ■

Remark 1 (Relevance of the Net Ripple Expression): It is worth noting the simplicity of Theorem 1, as depicted in Fig. 3, and the way in which it demonstrates that the net waveform is intimately dependent on the factor Nd. Specifically, the amplitude expression in (5) straightforwardly confirms the known property that the ripple undergoes complete cancellation when Nd is an integer. This property is captured simply by

Authorized licensed use limited to: University of Washington Libraries. Downloaded on February 10,2022 at 21:47:26 UTC from IEEE Xplore. Restrictions apply.

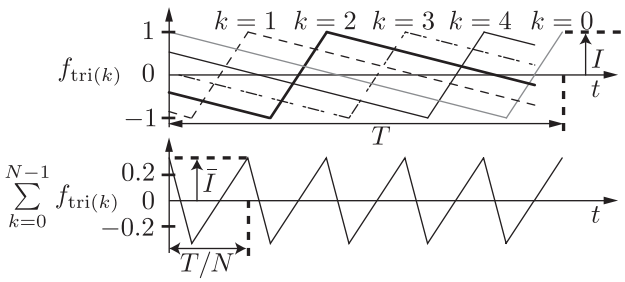

Fig. 4. Illustrative example of five interleaved waveforms. Top and bottom plots show the interleaved waveforms and the net waveform after superposition.

the fact that $\mathrm{mod}(Nd, 1) = 0$ if and only if $Nd \in \mathbb{Z}$. This interpretation using the modulo operator is unique to this work.

Numerical Example: Consider an illustrative case where $N = 5$ interleaved waveforms, each with duty ratio $d = 1/7$ and amplitude $I = 1$, are summed. The original waveforms and the net waveform after superposition are shown in the top and bottom plots of Fig. 4, respectively. Applying (5) and (6), the magnitude and effective duty ratio of the resultant waveform after superposition are $\bar{I} = 1/3$ and $\bar{d} = \mathrm{mod}(5/7, 1) \approx 0.71$, respectively. Equation (7) confirms the well-established outcome that the net waveform has an effective period that is reduced by a factor of $1/N$ in comparison to the individual waveforms before superposition.

IV. Experimental Results

To validate the derivations in Section III, we utilize the system in Fig. 5, which consists of $N = 3$ interleaved buck converters with a shared bipolar voltage source $\pm v_{\mathrm{dc}}$ at the input and an ac voltage source v_s at the output. The output inductance and resistance of each converter are denoted as L and r, respectively. This particular circuit and control structure was selected to produce a wide range of switching duty ratios over which Theorem 1 can be assessed. Toward that end, we utilize a sinusoidal current command $i^*(t) = \sqrt{2}I^* \sin(\omega_o t)$ that is provided identically to each converter with amplitude I^* and frequency ω_o. Correspondingly, the output voltage source provides a sinusoidal ac waveform $v_s(t) = \sqrt{2}V \sin(\omega_o t)$. Since $i^*(t)$ and $v_s(t)$ are in phase and have identical frequencies, this implies that each converter is commanded to provide $P^* := I^*V$ of real ac power at unity power factor. To ensure proper tracking at the fundamental ac frequency, we utilize a proportional resonant compensator of the form $G_i(s) = k_p + k_i s/(s^2 + \omega_o^2)$, where $s = \sigma + j\omega$. As shown in Fig. 5, the pulse width modulation (PWM) carriers are interleaved and can be expressed as $f_{\mathrm{tri}}(t - kT/N + \phi_{\mathrm{pwm}}, d_c, T)$ for $k = 0, 1, 2$, where T is the switching period, $d_c = 0.5$, which implies a symmetric triangular carrier shape, and ϕ_{pwm} accounts for a phase shift of the PWM carriers with respect to v_s. The controllers and PWM are executed on a Texas Instruments F28335 DSP, and the load voltage source v_s is provided by a grid-connected 2 : 1 step-down transformer. System parameters are in Table I.

Fig. 6 shows the measured waveforms after the system reaches steady state. As illustrated, each of the individual converter outputs has a relatively large ripple component. However,

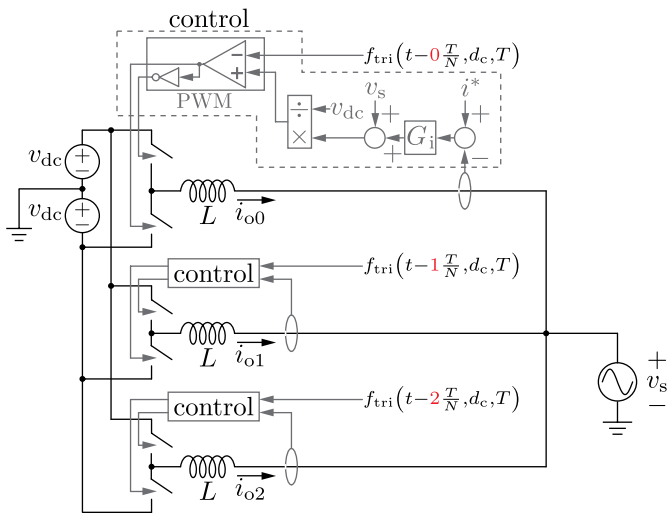

Fig. 5. Experimental setup consisting of three interleaved parallel-connected converters with current control.

TABLE I
Experimental Parameters

$L = 6\,\mathrm{mH}$	$T^{-1} = 10\,\mathrm{kHz}$	$\omega_o = 2\pi 60\,\mathrm{rad/s}$
$V = 65\,\mathrm{V}$	$I^* = 34/65\,\mathrm{A}$	$d_c = 0.5$
$r = 1\,\Omega$	$k_p = 7.5\,\mathrm{V/A}$	$k_i = 300\,\mathrm{V/(A \cdot s)}$
$v_{\mathrm{dc}} = 112.5\,\mathrm{V}$	$P^* = 34\,\mathrm{W}$	$Q^* = 0\,\mathrm{VAR}$

since the ripple components are interleaved, the total load current exhibits considerable ripple cancellation. To validate Theorem 1, we develop a model of the waveforms in Fig. 6 and compare the analytically computed result to the measurements. Along these lines, the kth sinusoidal steady-state output current is modeled as

$$i_{ok}(t) = i_{\mathrm{ac}}(t) + i_{\mathrm{r}k}(t) \tag{14}$$

where

$$i_{\mathrm{ac}}(t) = \sqrt{2}I_{\mathrm{ac}} \sin(\omega_o t) \tag{15}$$

is the low-frequency sinusoidal component and

$$i_{\mathrm{r}k}(t) = I(t) f_{\mathrm{tri}}\left(t - kT/N + \phi_{\mathrm{pwm}}, d(t), T\right) \tag{16}$$

encapsulates the triangular switching ripple. The decomposition of the current waveform into sinusoidal and ripple components facilitates analysis. Since the experiment was designed to ensure $L/r \gg T$, the ripple component can be approximated as a piecewise linear triangular function. Furthermore, since $G_i(j\omega)$ has infinite gain at $\omega = \omega_o$, we assume that each controller successfully tracks the sinusoidal current command such that $i_{\mathrm{ac}}(t) \to i^*(t) = \sqrt{2}I^* \sin(\omega_o t)$ asymptotically [14]. Taken together, these two assumptions substantiate the model in (14)–(16).

To characterize the ripple component in (16), we need to compute the ripple amplitude $I(t)$ and switching duty ratio $d(t)$. Leveraging a piecewise linear approximation for the inductor current and assuming volt-second balance, the ripple amplitude can be expressed as

$$I(t) = \frac{Td(t)}{2L}\left(v_{\mathrm{dc}} - |v_s(t)|\right). \tag{17}$$

Authorized licensed use limited to: University of Washington Libraries. Downloaded on February 10,2022 at 21:47:26 UTC from IEEE Xplore. Restrictions apply.

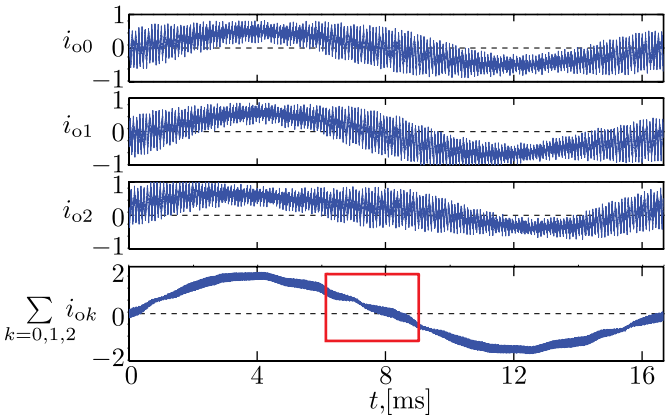

Fig. 6. Measured current for the interleaved converters and the total load current.

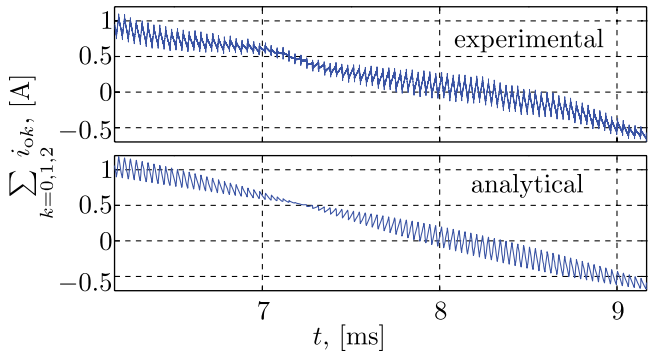

Fig. 7. Comparison of measured versus analytical waveforms for summed interleaved currents.

Using the classical relations for ac power flow across a line in conjunction with the parameters in Table I, it is straightforward to show that $d(t)$ converges to $1/2 + X\sin(\omega_o t + Y)$ in steady state where the values $X \approx 0.409$ and $Y \approx 18.2 \times 10^{-3}$ rad ensure that the commands P^* and Q^* are satisfied. Substituting (17) and the steady-state expression for $d(t)$ into (16), the analytical model for the kth current in (14) is complete. Accordingly, the total load current is now modeled by

$$\begin{aligned}\sum_{k=0}^{2} i_{ok}(t) &= 3\sqrt{2}I_{\rm ac}\sin(\omega_o t) \\ &\quad + \sum_{k=0}^{2} I(t) f_{\rm tri}\left(t - \frac{kT}{N} + \phi_{\rm pwm}, d(t), T\right) \\ &= 3\sqrt{2}I_{\rm ac}\sin(\omega_o t) + \bar{I} f_{\rm tri}(t + \phi_{\rm pwm}, \bar{d}, \bar{T}) \quad (18)\end{aligned}$$

where Theorem 1 was used to write the ripple summation as a single triangular waveform with parameters $\bar{I}$, $\bar{d}$, and $\bar{T}$, which are, in turn, specified by (5)–(7).

To compare the analytical model with measurements, focus on the segment enclosed by the red box in Fig. 6. Referring to Fig. 7, the measured load current is reproduced in up-close detail alongside a plot of the analytical expression in (18). A comparison of the waveforms confirms that the analytically computed result from Theorem 1 not only captures the summed ripple amplitude but also describes the effective duty ratio across the ac cycle and effective switching period, thus confirming the validity of our main result under dynamic conditions. In summary, Theorem 1 provides a comprehensive time–domain description of the net-ripple waveform.

V. Concluding Remarks

Leveraging modular arithmetic and Fourier series, we derived an analytical model that comprehensively describes the superposition of N interleaved triangular waveforms. The main result is presented with a level of generality such that it can be used to analyze interleaved triangular waveforms in a variety of energy conversion circuits. Specifically, it was shown that the superposition of N interleaved triangular waveforms with identical amplitudes and duty ratios is exactly to equal another single triangular waveform whose net amplitude, effective duty ratio, and effective frequency can be specified in terms of the original parameters in closed form. Our analysis was validated experimentally in a system consisting of three parallel converters.

References

[1] D. Perreault and J. Kassakian, "Distributed interleaving of paralleled power converters," *IEEE Trans. Circuits Syst. I, Reg. Papers*, vol. 44, no. 8, pp. 728–734, Aug. 1997.

[2] P.-W. Lee, Y.-S. Lee, D. Cheng, and X.-C. Liu, "Steady-state analysis of an interleaved boost converter with coupled inductors," *IEEE Trans. Ind. Electron.*, vol. 47, no. 4, pp. 787–795, Aug. 2000.

[3] K.-W. Hu, J.-C. Wang, T.-S. Lin, and C.-M. Liaw, "A switched-reluctance generator with interleaved interface dc-dc converter," *IEEE Trans. Energy Convers.*, vol. 30, no. 1, pp. 273–284, Mar. 2015.

[4] O. Garcia, P. Zumel, A. de Castro, and J. Cobos, "Automotive dc-dc bidirectional converter made with many interleaved buck stages," *IEEE Trans. Power Electron.*, vol. 21, no. 3, pp. 578–586, May 2006.

[5] B. Miwa, D. Otten, and M. Schlecht, "High efficiency power factor correction using interleaving techniques," in *Proc. Appl. Power Electron. Conf. Expo.*, Feb. 1992, pp. 557–568.

[6] B. Miwa, "Interleaved conversion techniques for high density power supplies," M.S. thesis, Dept. Electr. Eng. Comput. Sci., Massachusetts Inst. Technol., Boston, MA, USA, May 1992.

[7] C. Chang and M. Knights, "Interleaving technique in distributed power conversion systems," *IEEE Trans. Circuits Syst. I, Fundam. Theory Appl.*, vol. 42, no. 5, pp. 245–251, May 1995.

[8] S. Ozeri, D. Shmilovitz, S. Singer, and L. Martinez-Salamero, "The mathematical foundation of distributed interleaved systems," *IEEE Trans. Circuits Syst. I, Reg. Papers*, vol. 54, no. 3, pp. 610–619, Mar. 2007.

[9] C. Casablanca and J. Sun, "Interleaving and harmonic cancellation effects in modular three-phase voltage-sourced converters," in *Proc. IEEE Workshops Comput. Power Electron.*, Jul. 2006, pp. 275–281.

[10] M. Schuck and R. Pilawa-Podgurski, "Ripple minimization through harmonic elimination in asymmetric interleaved multiphase dc-dc converters," *IEEE Trans. Power Electron.*, vol. 30, no. 12, pp. 7202–7214, Dec. 2015.

[11] O. Garcia, A. de Castro, P. Zumelis, and J. Cobos, "Digital-control-based solution to the effect of nonidealities of the inductors in multiphase converters," *IEEE Trans. Power Electron.*, vol. 22, no. 6, pp. 2155–2163, Nov. 2007.

[12] S. Zhang and X. Yu, "A unified analytical modeling of the interleaved pulse width modulation (PWM) dc-dc converter and its applications," *IEEE Trans. Power Electron.*, vol. 28, no. 11, pp. 5147–5158, Nov. 2013.

[13] I. S. Gradshteyn and I. M. Ryzhik, *Table of Integrals, Series, and Products*. New York, NY, USA: Academic, 1980.

[14] R. Teodorescu, F. Blaabjerg, M. Liserre, and P. C. Loh, "Proportional-resonant controllers and filters for grid-connected voltage-source converters," *Proc. Inst. Elect. Eng.—Elect. Power Appl.*, vol. 153, no. 5, pp. 750–762, Sep. 2006.

Authorized licensed use limited to: University of Washington Libraries. Downloaded on February 10,2022 at 21:47:26 UTC from IEEE Xplore. Restrictions apply.